



Effect of Ce addition on the microstructure and damping properties of Cu–Al–Mn shape memory alloys

Xili Lu*, Feng Chen, Weishu Li, Yufeng Zheng

Center for Biomedical Materials and Engineering, Harbin Engineering University, Harbin 150001, PR China

ARTICLE INFO

Article history:

Received 29 October 2008

Received in revised form 23 January 2009

Accepted 30 January 2009

Available online 10 February 2009

Keywords:

Metals and alloys

Microstructure

Phase transitions

Thermodynamic properties

ABSTRACT

The effect of rare earth element Ce addition on the microstructure, martensitic transformation, mechanical properties and damping behavior of the Cu–Al–Mn shape memory alloys (SMAs) had been investigated. It is shown that the Ce addition makes the grain refinement and affects the martensitic transformation temperature. The tensile strength and the ductility of the Cu–Al–Mn alloys can be enhanced by the Ce addition. Damping capacity $\tan \delta$ of the martensite for the Cu–Al–Mn–Ce alloys is strain amplitude dependent. The Ce addition has obvious effects on the damping properties of the martensite. With the increase of the Ce content, the damping capacity increases initially and then decreases.

© 2009 Elsevier B.V. All rights reserved.

1. Introduction

Cu–Al–Mn shape memory alloys (SMAs) have attracted increasing attention because of their good shape memory effect, relatively low cost and good mechanical properties in addition to its outstanding damping capacity [1–5]. Several pioneering works have demonstrated that some characteristics such as superelasticity, shape memory effect and the damping properties in Cu–Al–Mn-based SMAs can be enhanced by the addition of alloying elements [6]. Sutou et al. [7] have reported that the addition of B, Ni, Si can reduce the grain size obviously. They also investigated the effects of grain size on the damping properties and found that grain size was very important for enhancement of the damping and mechanical properties. Mallik and Sampath [8] studied the influences of eight different elements as quaternary additions on the transformation temperatures, shape memory effects and superelasticity of Cu–Al–Mn alloys.

It is well known that rare earth elements are often used as alloying element to purify the grain boundary, refine the grains and improve the mechanical properties. Several rare earth elements (Ce, Gd, Dy, Tb and Sm) have been added to TiNi alloys, NiMnGa alloys and Cu–Zn–Al alloys [9–12] and some expected good results have been obtained. However, little information about rare earth Ce addition to Cu–Al–Mn alloys is found up to date. The purpose of the present work is to investigate the effect of rare earth element Ce on

the microstructure, mechanical properties and damping properties of the Cu–Al–Mn alloy.

2. Experimental procedure

(Cu₈₃Al₁₂Mn₅)_{1-x}Ce_x ($x=0, 0.05, 0.1$ and 0.15 wt%) alloys were prepared from high-purity elements (99.9% Cu, 99.9% Al and 99.9% Mn) in a non-consumed vacuum arc furnace under an argon atmosphere. Each ingot was remelted six times and then homogenized at 900 °C for 6 h. The master ingots were hot-rolled to sheets with the thickness of about 1.0 mm at 850 °C. All experimental specimens were spark-cut from the sheet and solution-treated at 850 °C for 2 h in an evacuated and sealed quartz capsules followed by quenched into water.

Optical microstructure observations were made using an Olympus optical metallographic microscope. The morphology, distribution and structure of the precipitated phase were determined by a HITACHI S-4700 scanning electron microscope (SEM) equipped with an energy dispersive X-ray spectroscopy (EDS) analysis system. The phase transformation temperatures were determined using a PerkinElmer Diamond DSC with a heating/cooling rate of 20 °C/min. Phase identification was performed in a Rigaku D/max-rB X-ray diffractometer (XRD) with Cu K α radiation.

Damping properties of the samples were characterized by a dynamic mechanical analyzer (TA Q800). Samples with a size of 36 mm \times 6 mm \times 1 mm were measured in single cantilever mode. The test was performed at room temperature and the frequency was 1 Hz, while the strain amplitude was in the range of 1×10^{-6} to 1×10^{-3} . To obtain a full martensite structure, the samples were firstly quenched into liquid nitrogen and then hold at room temperature (lower than the martensitic reverse transformation temperature).

3. Results and discussion

3.1. Microstructure and phase transformation of Cu–Al–Mn–Ce alloys

Fig. 1(a)–(d) shows the optical micrographs of (Cu₈₃Al₁₂Mn₅)_{1-x}Ce_x alloys. Obviously, the grain size is clearly

* Corresponding author. Tel.: +86 451 82518173; fax: +86 451 82518644.
E-mail address: lusissi1975@126.com (X. Lu).

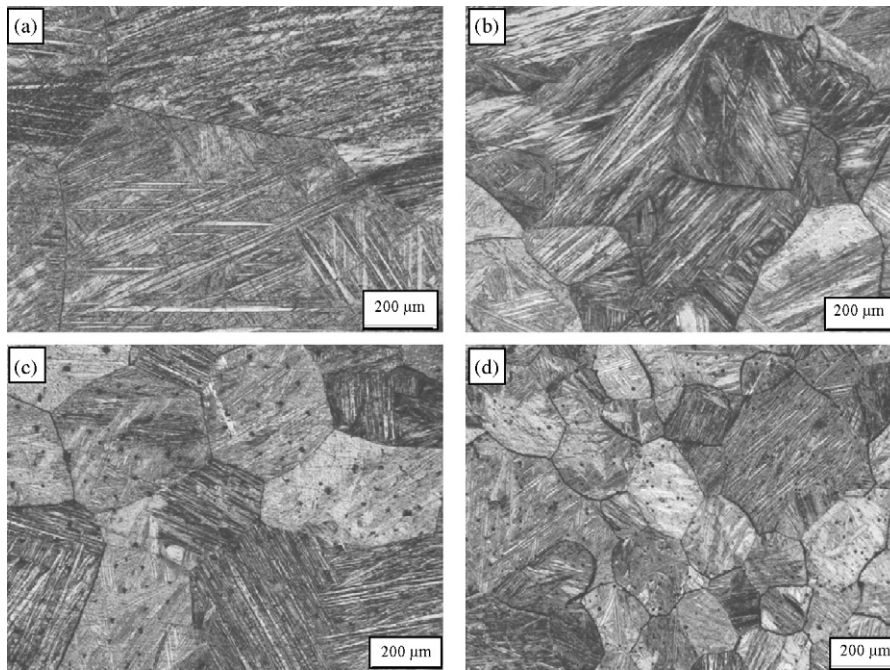


Fig. 1. Optical micrographs of solution-treated $(\text{Cu}_{83}\text{Al}_{12}\text{Mn}_5)_{1-x}\text{Ce}_x$ alloys (a) $x=0$, (b) $x=0.05$, (c) $x=0.1$ and (d) $x=0.15$.

reduced with the increase of Ce content. In addition, the addition of Ce markedly changes the microstructure of the $\text{Cu}_{83}\text{Al}_{12}\text{Mn}_5$ alloy. The ternary $\text{Cu}_{83}\text{Al}_{12}\text{Mn}_5$ alloy exhibits a single martensite phase, whereas all the Ce-doped quaternary alloys contain a second phase (black dots inside each grain) besides the martensite phase, as shown in Fig. 1. When $x=0.05$, very small amounts of the second phase disperse in the matrix. With the increase of the Ce content, the volume fraction of the second phase increases gradually. It is worth noting that the variant interfaces in the martensite shows the trend to parallel one to another in each grain with the existing of the second phase. This microstructural feature suggests that these martensite variant interfaces have high mobility [8].

Fig. 2 illustrates the typical backscattered electron image and the corresponding EDS spectrum for the second phase in the $(\text{Cu}_{83}\text{Al}_{12}\text{Mn}_5)_{99.85}\text{Ce}_{0.15}$ alloy. The results show that the content of Ce in the precipitated phase reaches 19.58 wt%, the content of other elements are 61.71 wt% Cu, 17.36 wt% Al and 1.35 wt% Mn, respectively. Compared with the composition of the matrix, the second phase has a larger concentration of Ce, which means that the solubility of Ce in the matrix is very low and the insoluble Ce forms the Ce-rich phase. The reason for the formation of Ce-rich phase in

Cu–Al–Mn alloys may be explained as follows: the atomic radius of Ce is much larger than that of Cu, Al and Mn, which means that the solubility of Ce in the matrix is very low. Insoluble Ce element gets enriched at the interface between the solid and the liquid during the cooling process, which will be favor of the formation of Ce-rich phase. Further details of the Ce-rich phase are under investigation.

The X-ray diffraction patterns of the experimental alloys are shown in Fig. 3. As compared with those published in the literature [13,14], the peaks in the patterns are identified. It can be seen that both β_1' and γ_1' martensites are present in all the alloys. It is worth noting that the amount of β_1' martensite increases with the increase of the Ce content and reaches a maximum at 0.1 wt% Ce content, then the amounts of β_1' martensite decrease as the Ce content increases further. The existence of different martensite variants leads to more phase interfaces and twin boundaries.

Fig. 4 shows the DSC curves of the $(\text{Cu}_{83}\text{Al}_{12}\text{Mn}_5)_{1-x}\text{Ce}_x$ alloys. It can be seen that there is only one endothermic or one exothermic peak in the heating or cooling DSC curves, respectively. This indicates that the Cu–Al–Mn–Ce alloys maintain the characteristics of the typical one-step thermoelastic martensitic transformation of $\text{Cu}_{83}\text{Al}_{12}\text{Mn}_5$ alloy. The addition of Ce affects the phase transfor-

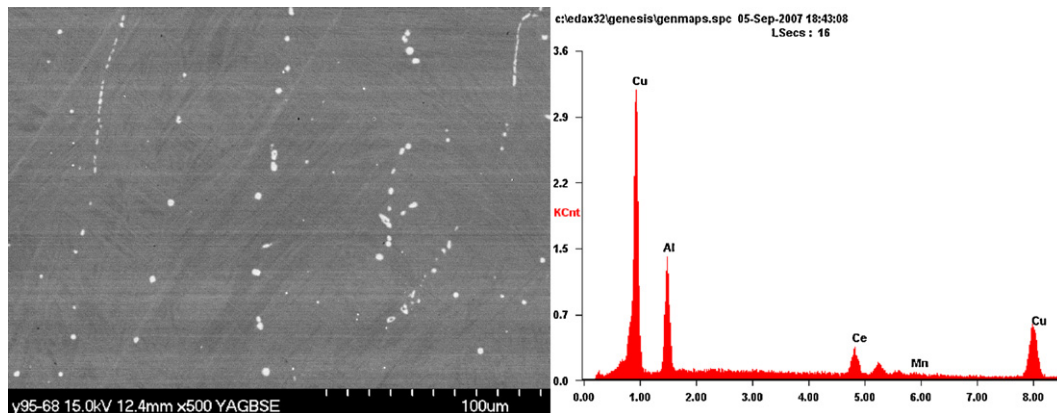


Fig. 2. (a) Morphology of Ce-rich phase and (b) the corresponding EDS spectrum in the $(\text{Cu}_{83}\text{Al}_{12}\text{Mn}_5)_{99.85}\text{Ce}_{0.15}$ alloy.

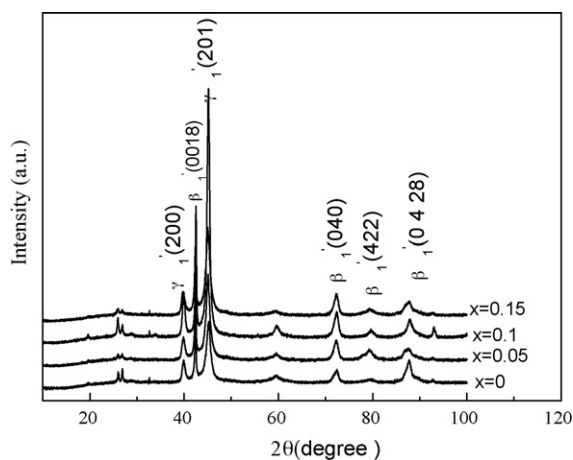


Fig. 3. X-ray diffraction patterns of $(\text{Cu}_{83}\text{Al}_{12}\text{Mn}_5)_{1-x}\text{Ce}_x$ ($x=0, 0.05, 0.1$ and 0.15) alloys at room temperature.

mation temperature of the $(\text{Cu}_{87}\text{Al}_{12}\text{Mn}_5)_{1-x}\text{Ce}_x$ alloys. With the increase of the Ce content, the martensitic transformation temperatures (M_s and M_f) decrease firstly, and the lowest value of M_s and M_f is obtained while the content of Ce reaches 0.1%. However, the M_s and M_f temperatures increase with further increasing the Ce content. Two contributions maybe account for these phenomena. One originates from the formation of the Ce-rich phase, which causes the change of composition of matrix. According to the EDS results, the Ce-rich phase contains smaller amounts of Mn and more amounts of Al, which leads to richness of Mn and leanness of Al in the matrix. It is known that the M_s temperature decreases with the increase of the content of Mn and Al, and the Mn content can affect more than Al content on the M_s temperature. Therefore, the addition of Ce makes the M_s temperature decrease. And the other arises from the existence of different amounts of two kind of martensites in the matrix [15].

3.2. Mechanical properties of Cu–Al–Mn–Ce alloys

Fig. 5 displays the stress–strain curves of $(\text{Cu}_{83}\text{Al}_{12}\text{Mn}_5)_{1-x}\text{Ce}_x$ alloys at room temperature. It is seen that the tensile strength of CuAlMn alloy is obviously enhanced by the Ce addition. The highest tensile strength is obtained in $(\text{Cu}_{83}\text{Al}_{12}\text{Mn}_5)_{99.95}\text{Ce}_{0.05}$ alloy, nearly 890 MPa. This value is about 300 MPa higher than that of the alloy without the Ce addition. Additionally, it is noted that the addition of Ce improves the ductility. The elongation of CuAlMn alloy increases gradually with increasing Ce content. These results prove

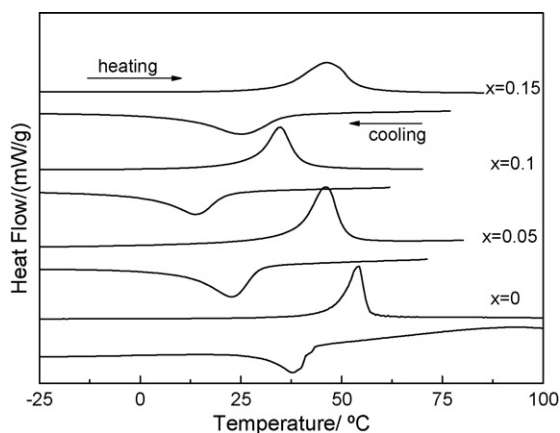


Fig. 4. DSC curves of $(\text{Cu}_{83}\text{Al}_{12}\text{Mn}_5)_{1-x}\text{Ce}_x$ ($x=0, 0.05, 0.1$ and 0.15) alloys as solution-treated.

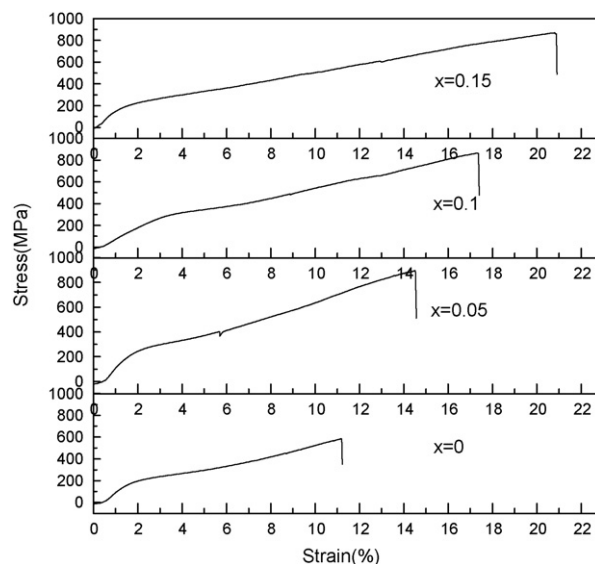


Fig. 5. The stress–strain curves of $(\text{Cu}_{83}\text{Al}_{12}\text{Mn}_5)_{1-x}\text{Ce}_x$ ($x=0, 0.05, 0.1$ and 0.15) alloys under martensite condition.

that the proper amount of Ce addition significantly enhances the tensile strength and improves the ductility of the alloys.

3.3. Damping properties of Cu–Al–Mn–Ce alloys

In order to investigate the effect of rare earth element Ce on the damping properties, the dynamic thermal analysis tests were carried out in the martensite condition. As we known, the damping capacity during phase transformation is not of the intrinsic value, strongly depending on the cooling/heating rate, so the damping capacity in the martensite condition is more essential and important for evaluation of the damping properties. Thus, this work focuses on the effect of Ce addition on the damping properties of martensite for $\text{Cu}_{83}\text{Al}_{12}\text{Mn}_5$ alloy. Fig. 6(a) demonstrates the evolution of the damping capacity $\tan \delta$ as a function of strain amplitude in the martensite condition for the $(\text{Cu}_{83}\text{Al}_{12}\text{Mn}_5)_{1-x}\text{Ce}_x$ alloys. It is seen that the damping capacity $\tan \delta$ of the martensite increases gradually with an increase of strain amplitude for each alloy. It also can be seen that the damping capacity $\tan \delta$ of the martensite is obviously affected by Ce addition. With the increase of the Ce content, the damping capacity $\tan \delta$ increases initially and then decreases. The highest damping capacity $\tan \delta$ is obtained in the $(\text{Cu}_{83}\text{Al}_{12}\text{Mn}_5)_{99.95}\text{Ce}_{0.05}$ alloy. Fig. 6(b) shows the effect of strain amplitude on the storage modulus of $(\text{Cu}_{83}\text{Al}_{12}\text{Mn}_5)_{1-x}\text{Ce}_x$ alloys with different Ce addition. The storage modulus of $(\text{Cu}_{83}\text{Al}_{12}\text{Mn}_5)_{1-x}\text{Ce}_x$ alloys is obviously enhanced by the Ce addition. In addition, it is worth noting that the $(\text{Cu}_{83}\text{Al}_{12}\text{Mn}_5)_{99.95}\text{Ce}_{0.05}$ alloy possesses the highest storage modulus.

It is generally accepted that the self-accommodation of martensitic plates and a high density of mobile twins in the martensite condition lead to high damping capacity of the martensite of the alloys [16]. Thus, the experimental results can be explained as follows: on the one hand, when rare earth Ce is added to Cu–Al–Mn alloy, Ce is easy to react with the impure elements and can purify the liquid alloy, which can decrease the inherence of the movements of martensite variant interfaces. Meanwhile, according to the results of optical micrograph, the martensite variant oriented due to the Ce addition, which leads to the improvement of the interface mobility. Additionally, the number of martensite variant interfaces increase due to the existing different type of martensite, as indicated by XRD results. Therefore, the damping capacity of the

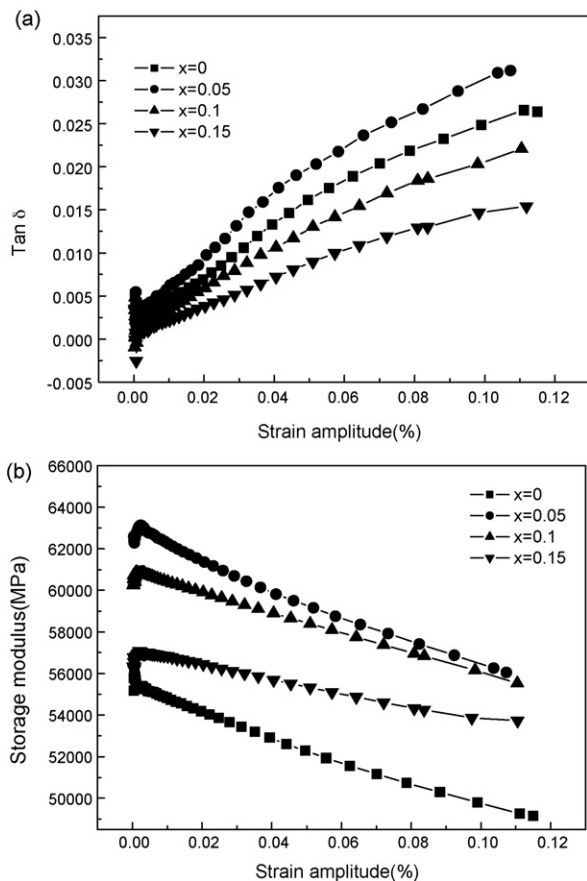


Fig. 6. The effect of strain amplitude on (a) $\tan \delta$ and (b) storage modulus of $(\text{Cu}_{83}\text{Al}_{12}\text{Mn}_5)_{1-x}\text{Ce}_x$ ($x = 0, 0.05, 0.1$ and 0.15) alloys.

martensite is enhanced by means of increasing the mobility and the number of martensite variant interfaces. On the other hand, as mentioned above, the grain size of $(\text{Cu}_{83}\text{Al}_{12}\text{Mn}_5)_{1-x}\text{Ce}_x$ alloys decrease obviously, thus, the mobility of interfaces can be restricted by the grain boundary. The decrease of the mobility of martensite variant interfaces due to an increment of the grain constraint can lead to the decrement of the damping capacity. In addition, the size and distribution of Ce-rich phase play important roles in affecting the damping properties of the martensite for $(\text{Cu}_{83}\text{Al}_{12}\text{Mn}_5)_{1-x}\text{Ce}_x$ alloys. With the increase of Ce content, the Ce-rich phase grows and the volume fraction of the precipitated phase increases gradually. The existence of the Ce-rich phase hinders effectively the movement of the boundaries between martensite variants and twin boundaries, which results in the decrease of the damping capacity. As discussed above, it can be concluded that there exists an appro-

appropriate amount of Ce addition content for achieving a maximum damping capacity for the Cu–Al–Mn alloy. Combining the tensile test results, the $(\text{Cu}_{83}\text{Al}_{12}\text{Mn}_5)_{99.95}\text{Ce}_{0.05}$ alloy exhibit both high damping capacity and high strength. Therefore, it can be concluded that a certain amount of Ce addition not only improves the damping capacity but also enhances the strength of martensite, which is very useful for engineering applications.

4. Conclusions

The effect of Ce addition on the microstructure, phase transformation, mechanical properties and damping properties of $(\text{Cu}_{83}\text{Al}_{12}\text{Mn}_5)_{1-x}\text{Ce}_x$ alloys is studied. The results show that the Ce doping refines obviously the grains and causes the formation of Ce-rich phase. With the increase of Ce content, the Ce-rich phase becomes larger and the volume fraction increases gradually. The martensitic transformation type cannot be affected by the Ce addition. However, the phase transformation temperatures firstly decrease and then increase with the Ce content increasing. The mechanical properties of the $\text{Cu}_{83}\text{Al}_{12}\text{Mn}_5$ alloy are improved by the Ce addition. In addition, appropriate Ce doping can enhance the damping capacity of the martensite for Cu–Al–Mn alloy and the $(\text{Cu}_{83}\text{Al}_{12}\text{Mn}_5)_{99.95}\text{Ce}_{0.05}$ alloy possesses the best damping capacity and the tensile strength.

Acknowledgements

This work was supported by China Postdoctoral Science Foundation and the School Foundation of Harbin Engineering University (HEUFT07045).

References

- [1] N. Zárubová, V. Novák, Mater. Sci. Eng. A 378 (2004) 216.
- [2] U.S. Mallik, V. Sampath, Mater. Sci. Eng. A 478 (2008) 48–55.
- [3] Y. Zheng, C. Li, F. Wan, Y. Long, J. Alloys Compd. 441 (2007) 317–321.
- [4] Q.Z. Wang, F.S. Han, J. Wu, G.L. Hao, Z.Y. Gao, J. Alloys Compd. 425 (2006) 200–205.
- [5] Y. Sutou, T. Omori, K. Yamauchi, N. Ono, R. Kainuma, K. Ishida, Acta Mater. 53 (2005) 4121–4133.
- [6] Y. Sutou, T. Omori, J.J. Wang, R. Kainuma, K. Ishida, Mater. Sci. Eng. A 378 (2004) 278–282.
- [7] Y. Sutou, T. Omori, N. Koeda, R. Kainuma, K. Ishida, Mater. Sci. Eng. A 438–440 (2006) 743–746.
- [8] U.S. Mallik, V. Sampath, J. Alloys Compd. (2008), doi:10.1016/j.jallcom.2008.01.128.
- [9] A.L. Liu, Z.Y. Gao, L. Gao, W. Cai, Y. Wu, J. Alloys Compd. 437 (2007) 339–343.
- [10] W. Cai, L. Gao, A.L. Liu, J.H. Sui, Z.Y. Gao, Scripta Mater. 57 (2007) 659–662.
- [11] Z.Q. Zhao, W. Xiong, S.X. Wu, X.L. Wang, J. Iron Steel Res. 111 (2004) 55–61.
- [12] J.W. Xu, J. Alloys Compd. 448 (2008) 331–335.
- [13] R. Kainuma, S. Takahashi, K. Ishida, Metall. Mater. Trans. A 27A (1996) 2187–2195.
- [14] R.H. Wang, J.N. Guo, X.M. Chen, S.S. Tan, Acta Mater. 50 (2002) 1835–1847.
- [15] U.S. Mallik, V. Sampath, J. Alloys Compd. 459 (2008) 142–147.
- [16] J. Van Humbeeck, J. Alloys Compd. 355 (2003) 58–64.